Available online at www.sciencedirect.com
ScienceDirect
Journal of Crystal Growth 308 (2007) 412–416
JOURNAL OF CRYSTAL GROWTH
www.elsevier.com/locate/jcrysgro

Growth and characterization of nonpolar ZnO (1 0 $\bar{1}$ 0) epitaxial film on γ-$LiAlO_2$ substrate by chemical vapor deposition

Mitch M.C. Chou[a,*], Liuwen Chang[a], Hsiao-Yi Chung[a], Teng-Hsing Huang[a], Jih-Jen Wu[b], Chun-Wei Chen[c]

[a]*Department of Materials Science and Opto-electronic Engineering, National Sun Yat-Sen University, Kaohsiung 80424, Taiwan*
[b]*Department of Chemical Engineering, National Cheng Kung University, Tainan 701, Taiwan*
[c]*Department of Materials Science and Engineering, National Taiwan University, Taipei 106, Taiwan*

Received 25 March 2007; received in revised form 15 June 2007; accepted 22 August 2007
Communicated by R. Bhat
Available online 30 August 2007

Abstract

A simple chemical vapor deposition approach to the growth of nonpolar ZnO with [1 0 $\bar{1}$ 0] orientation on a γ-$LiAlO_2$ substrate is presented. The dependence of growth characteristics on the growth temperature is investigated. Following the CVD growth, the surface morphologies of ZnO film were investigated by a scanning electron microscope. The characterizations of structure and orientation by a scanning transmission electron microscope indicate that the ZnO film is oriented in the nonpolar [1 0 $\bar{1}$ 0] *m*-direction. Photoluminescence result of nonpolar ZnO shows a strong UV emission peak at around 375 nm at room temperature.

PACS: 71.20.Nr; 73.61.Ga

Keywords: A2. Czochralski method; A3. Chemical vapor deposition; B1. Zinc compounds

1. Introduction

The wide-bandgap semiconductor ZnO having the wurtzite structure is attractive for application in ultraviolet (UV) light-emitting devices (LED) [1,2]. It is also a candidate for use in piezoelectric devices [3]. The growth of ZnO films was conventionally conducted on *c*-plane Al_2O_3 substrates, because hexagonal ZnO grows preferentially along the [0 0 0 1] growth direction. However, wurtzite-type materials, like GaN and ZnO exhibit a strong lattice polarization effect along the *c*-axis leading to built-in electric fields in wells and barriers of multi-quantum well (MQW) structures [4]. This internal electric field in MQW structures separates electron and hole wave functions in real space, which leads to spatially indirect optical transitions for UV-emitting LEDs and lower quantum efficiencies for radiative transitions. This so-called quantum confined stark effect (QCSE), which is well established for GaN-based heterostructures, also causes an undesirable red shift in the emission spectra of MQW structures designed for UV emission [5]. Recently, this effect was also found in ZnO/ZnMgO QW structure [6]. In order to overcome these problems, it is proposed to grow ZnO films along nonpolar directions, such as (1 1 $\bar{2}$ 0) (*a*-plane) [7,8], (1 0 $\bar{1}$ 0) (*m*-plane) [9,10], and {2 1 $\bar{1}$ 0} (*r*-plane) [11–13]. Zuniga-Perez et al. [7,10] used metal organic vapor-phase epitaxy (MOVPE) to grow *m*-plane ZnO on (1 0 $\bar{1}$ 0) Al_2O_3 and studied the polarity effects. Fujita et al. also used MOVPE on (1 0 $\bar{1}$ 0) Al_2O_3 substrates to obtain *m*-plane ZnO film [11]. They found that higher growth temperature (500–800 °C) and higher mole fractions of oxygen to zinc precursors lead to the growth of nonpolar ZnO films. When both the growth temperature and the VI/II mole fraction were decreased, (0 1 $\bar{1}$ 3) ZnO

*Corresponding author.
E-mail addresses: mitch@mail.nsysu.edu.tw (M.M.C. Chou), lwchang@mail.nsysu.edu.tw (L. Chang), brief1126@hotmail.com (H.-Y. Chung), m953060004@student.nsysu.edu.tw (T.-H. Huang), wujj@mail.ncku.edu.tw (J.-J. Wu), chunwei@ntu.edu.tw (C.-W. Chen).

0022-0248/$ - see front matter © 2007 Elsevier B.V. All rights reserved.
doi:10.1016/j.jcrysgro.2007.08.019

started to form. Matsui and Tabata [12,13] reported on ZnO homoepitaxy on (1 0 $\bar{1}$ 0) ZnO single-crystal substrates by molecular beam epitaxy (MBE). They found that small islands elongated along the {0 0 0 1} direction were generated on two-dimensional (2D) growth surfaces above a critical thickness and then they developed to [1 0 $\bar{1}$ 0] nanostripe arrays.

The previous works indicate that the selection of a proper substrate is important to achieve control of growth direction of ZnO films. Lattice match between the substrate and ZnO is one important criterion for successful growth, but in addition to the structural matching the chemical and thermal matching as well as the surface preparation play important roles in the growth direction and morphologies of ZnO films. The lattice mismatch between ZnO and Al_2O_3 is as large as 18%, which results in the considerable misfit strain and dislocations in the ZnO epitaxial layers. On the other hand, ZnO single crystals grown by the hydrothermal method are expensive, especially for the nonpolar ZnO surface orientation. In this paper, we report on the growth of nonpolar ZnO films on γ-$LiAlO_2$ substrates by chemical vapor deposition.

γ-$LiAlO_2$ has a tetragonal structure where the *a*–*c* (1 0 0) plane has the same atomic arrangement as the prismatic face (1 0 $\bar{1}$ 0) plane of the wurtzite structure. From the viewpoint of lattice mismatch between ZnO and $LiAlO_2$, $[0\,0\,1]_{LiAlO_2}//[1\,1\,\bar{2}\,0]_{ZnO}$, $c_{LiAlO_2}(6.278\,\text{Å}) \cong 2a_{ZnO}$ (3.252 Å) with 3.47% mismatch. $[0\,1\,0]_{LiAlO_2}//[0\,0\,0\,1]_{ZnO}$, $a_{LiAlO_2}(5.167\,\text{Å}) \cong c_{ZnO}(5.313\,\text{Å})$ with 2.71% mismatch. It can be clearly seen why the ZnO hexagonal cell is in the (1 0 $\bar{1}$ 0) or *m*-plane orientation which places the polar *c*-axis on the $LiAlO_2$ wafer plane (Fig. 1). This orientation will remove the influence of the electrostatic fields on ZnO and eliminate the problems of low electron–hole recombination probabilities due to QCSE. However, $LiAlO_2$ has several problems: $LiAlO_2$ single crystal can be grown by Czochralski pulling method, but it is difficult to obtain high quality crystal because Li atoms continue evaporating during the growth and cooling process. This leads to the nonstoichiometric ratio of the materials. Since $LiAlO_2$ reacts with water and most of the polishing solutions, it is difficult to obtain an atomic-flat surface. We already developed the methods of growing and polishing $LiAlO_2$ single crystal [14,15].

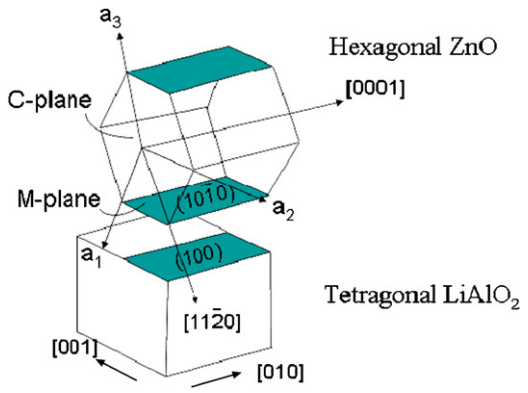

Fig. 1. ZnO hexagonal cell is in the (1 0 $\bar{1}$ 0) or *m*-plane orientation which places the polar *c*-axis on the $LiAlO_2$ wafer plane.

2. Experimental process

Here we present a simple chemical vapor deposition (CVD) approach to the growth of nonpolar ZnO with (1 0 $\bar{1}$ 0) orientation (*m*-plane) on a γ-$LiAlO_2$ single-crystal substrate. The dependence of growth characteristics on the growth temperature was investigated. Following the CVD growth, the surface morphologies of ZnO film were investigated by a scanning electron microscope (SEM). The characterizations of structure and orientation by X-ray diffraction pattern (XRD), and transmission electron microscope (TEM) indicate that ZnO film is oriented in the nonpolar [1 0 $\bar{1}$ 0] *m*-direction. Photoluminescence (PL) result of nonpolar ZnO shows a strong UV emission peak at around 375 nm at room temperature.

Nonpolar ZnO epitaxial films were grown in a two-temperature zone furnace. Zinc acetylacetonate hydrate

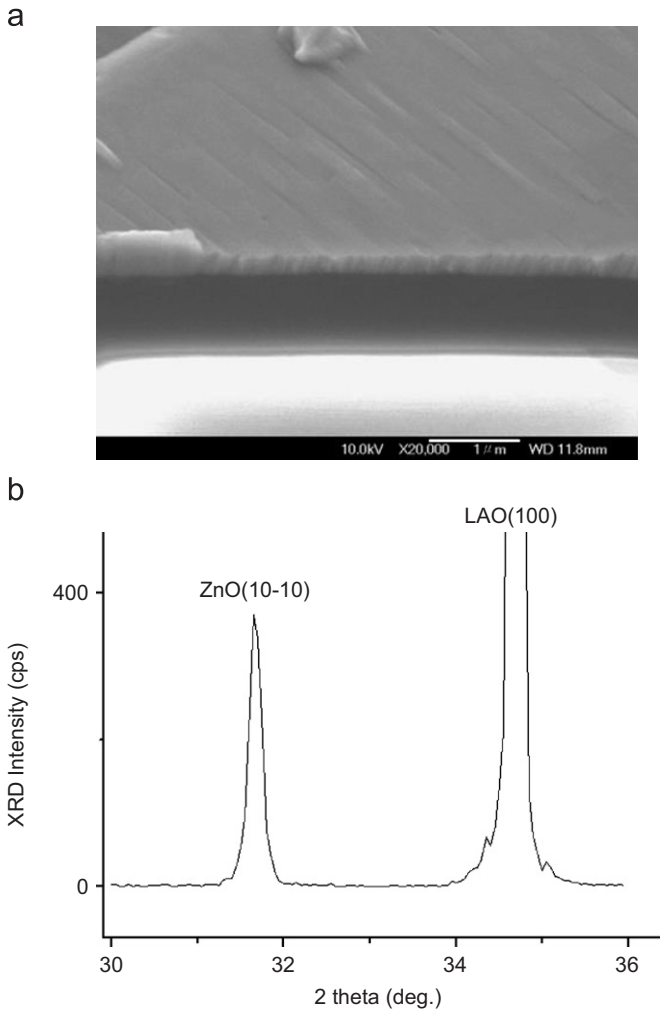

Fig. 2. SEM images of nonpolar ZnO grown at the growth temperature 650 °C. (a) 45° tilted view of ZnO surface, (b) XRD pattern on ZnO epitaxial film.

($Zn(C_5H_7O_2)_2 \cdot xH_2O$, Lancaster) was used for zinc source which was vaporized at 130–140 °C. The carrier gas was oxygen with 400 sccm flow rate and the chamber pressure was controlled at 200 Torr. Without any buffer layer, ZnO epitaxial films were directly grown on [1 0 0] $LiAlO_2$ single-crystal substrate at temperature of 550–650 °C for 1 h. Surface morphologies were examined using the JEOL JSM-6330TF SEM.

3. Results and discussion

Fig. 2(a) is a 45° tilted SEM image of ZnO epilayers grown on [1 0 0] $LiAlO_2$ substrate at temperature 650 °C. The films are quite uniform in the average thickness of 200 nm throughout the sample. Its orientation is identified as (1 0 $\bar{1}$ 0) *m*-plane by XRD (Fig. 2(b).

Further structural characterization of nonpolar ZnO epilayer was performed using TEM. Cross-sectioned TEM samples were prepared using the focus ion beam (SMI 3050) lift-out method [16]. A Ti layer of about 100 nm thick was pre-deposited on the sample to prevent charging. A thin sliver was then cut out of the specimen, with its surface normal parallel to the stripe direction, and was loaded on a carbon-coated grid. A JEOL 3010 scanning transmission electron microscope (STEM) operated at 200 kV was employed to characterize the microstructures and orientation of the nonpolar ZnO film. Fig. 3(a) show a cross-sectional bright-field image of the nonpolar ZnO grown on [1 0 0] $LiAlO_2$ substrate at a growing temperature of 650 °C. The image is taken near [$\bar{2}$ 1 1 0] zone axis with $\boldsymbol{g} = 000\bar{2}$. Both the interface and the surface are smooth. Strain contrast is observed in the substrate near the interface, indicating good lattice continuity is maintained. Fig. 3(b) shows the corresponding selected-area electron diffraction (SAED) patterns taken from the interface between ZnO and $LiAlO_2$. The incident beam is parallel to $[\bar{2}\,1\,1\,0]_{ZnO}$ and $[0\,0\,1]_{LiAlO_2}$ zone axes. Epitaxial relationship between ZnO and $LiAlO_2$ is thus determined as $[1\,0\,\bar{1}\,0]_{ZnO}//[1\,0\,0]_{LiAlO_2}$ and $[1\,1\bar{2}\,0]_{ZnO}//[0\,0\,1]_{LiAlO_2}$. These patterns provide direct evidences for the structural relationship of ZnO and $LiAlO_2$ substrate. Fig. 3(c) showed a high-resolution TEM image of the ZnO crystal along the [1 1 $\bar{2}$ 0] zone axis. The {0 0 0 2} ZnO crystal planes, which are perpendicular to the growth direction are clearly observable. The crystal planes running parallel to the growth direction are clearly observable. The measured inter-plane spacing (0.26 nm) matches well with the literature value for (0 0 0 2) planes in wurtzite ZnO—providing further confirmation that the ZnO film grows along the [1 $\bar{1}$ 0 0] direction.

The surface morphology of ZnO films are found to depend strongly on the growth temperature. The SEM

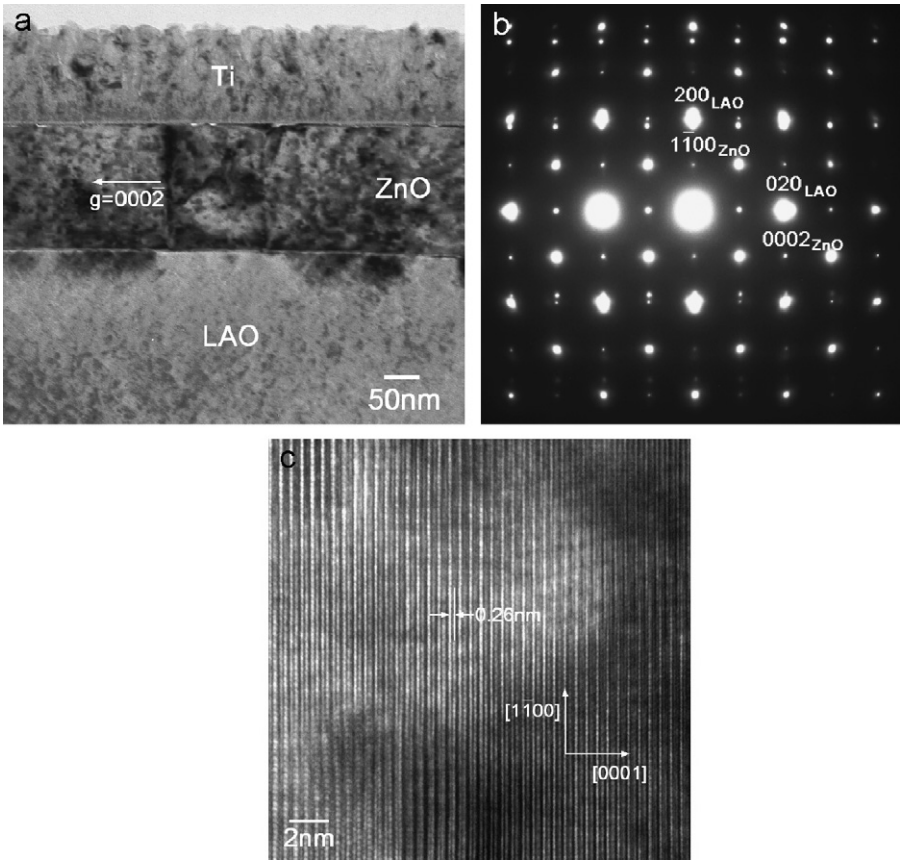

Fig. 3. (a) Cross-sectional bright field TEM image, (b) corresponding diffraction patterns, and (c) high-resolution image of the nonpolar ZnO grown on $LiAlO_2$ substrate at a growing temperature of 650 °C.

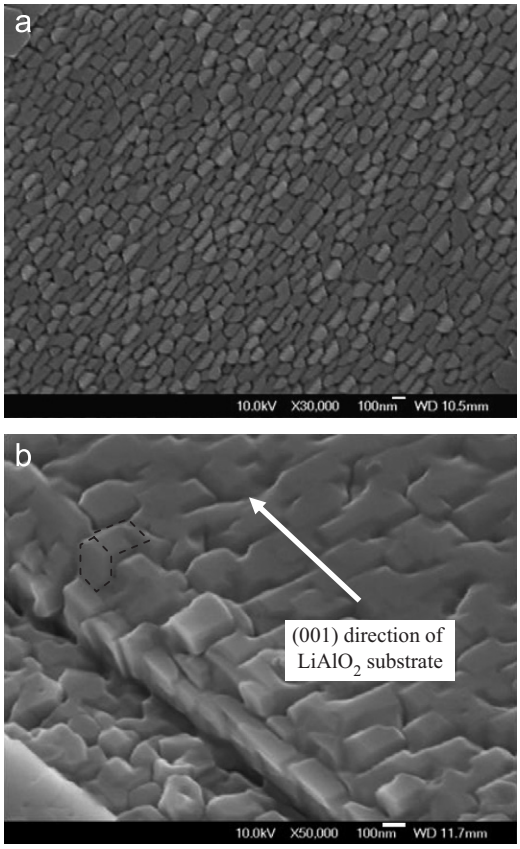

Fig. 4. SEM images of nonpolar ZnO grown at the growth temperatures of (a) 550 °C and (b) 600 °C.

image in Fig. 4(a) shows a high density of well-aligned ZnO dots with rectangular structure. The average size of ZnO dots is 80 nm × 120 nm and their height is about 50 nm. The size control of ZnO dots can be achieved by adjusting the position of the $LiAlO_2$ wafer in the growth chamber. The orientation of ZnO dots was identified as [1 0 $\bar{1}$ 0] *m*-direction by XRD. The SEM image also showed that ZnO has a higher growth rate in [1 0 $\bar{1}$ 0] direction which is perpendicular to $LiAlO_2$ substrate than lateral [0 0 0 1] direction at the growth temperature of 550 °C. When the growth temperature was raised to 600 °C, ZnO surface revealed many flaws between the rectangle-like blocks, (Fig. 4(b). It suggested that ZnO growth along [1 0 $\bar{1}$ 0] direction was suppressed a little at higher-growth temperature and the crystals started to grow sideways in the form of thin film. The relative growth rate along sideways is higher than [1 0 $\bar{1}$ 0] direction. ZnO hexagons, marked with the dashed line lay on the surface of $LiAlO_2$ substrate. The orientation of ZnO hexagons is the same as our assumption of Fig. 1.

The micro-PL (μPL) spectra were obtained by exciting the samples using a continuous wave (CW) He–Cd laser (325 nm) at room temperature and the emission spectra were collected and analyzed with a Jobin-Yvon TRIAX 550 monochromator with 0.025 nm resolution and detected by a photomultiplier tube and standard photocounting electronics. Fig. 5 shows the PL spectrum of the (1 0 $\bar{1}$ 0) *m*-plane ZnO grown on $LiAlO_2$ substrate at 650 °C. A strong UV emission at around 375 nm, and a wide band (450–600 nm) at the peak of 518 nm were observed. The UV emission is related to the direct recombination of photon-generated charge carriers. An additional green-band emission might be caused by the intrinsic defects and oxygen vacancy [17]. More oxygen vacancies would lead to the stronger intensity of the green emission. Since the green band is wide, it implied that the as-grown nonpolar ZnO has a high concentration of oxygen vacancies.

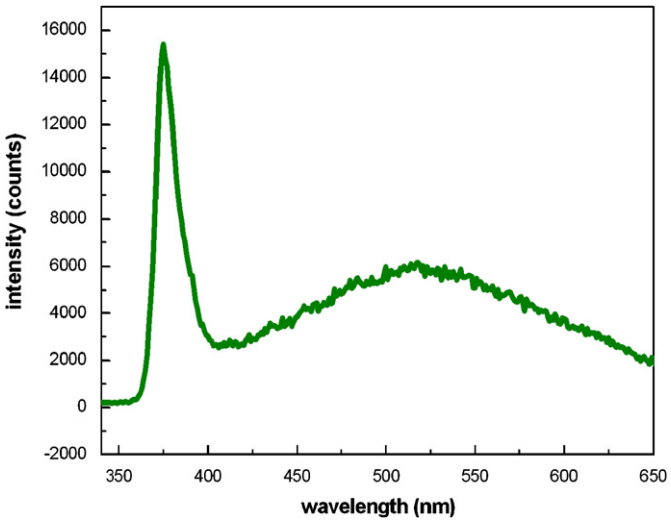

Fig. 5. Photoluminescence spectrum of nonpolar ZnO film grown on $LiAlO_2$ substrate at growth temperature 650 °C.

4. Conclusion

In conclusion, we have demonstrated the growth of nonpolar ZnO epitaxial film on [1 0 0] $LiAlO_2$ single-crystal substrate via thermal chemical vapor deposition. The ZnO films were oriented in [1 0 $\bar{1}$ 0] orientation (*m*-plane). The dependence of growth characteristics on the growth temperatures (550–650 °C) was investigated. It was found that the nonpolar ZnO films of uniform surface were obtained at the growth temperature 650 °C. TEM analysis provides direct evidence of the lattice-match growth mechanism of ZnO and $LiAlO_2$ substrate. The μPL spectrum of the (1 0 $\bar{1}$ 0) *m*-plane ZnO shows a strong UV emission peaking at around 375 nm. We believed that $LiAlO_2$ single-crystal substrate is a material potentially useful in nonpolar ZnO epitaxial growth.

Acknowledgments

This work is supported by NSC of Taiwan, NSC94-2218-E-110-008, ACORC, Aim for the Top University Plan and Center for Nanoscience & Nanotechnology of National Sun Yat-Sen University, Taiwan. Special thanks to Dr. Klaus Ploog for his valuable revisions.

References

[1] A. Tsukazaki, M. Kubota, A. Ohtomo, T. Onuma, K. Ohtani, H. Ohno, S.F. Chichibu, M. Kawasaki, Jpn. J. Appl. Phys. 44 (2005) L643.
[2] A. Tsukazaki, A. Ohtomo, T. Ohnuma, M. Ohtani, T. Makino, M. Sumiya, K. Ohtani, S.F. Chichibu, S. Fuke, Y. Segawa, H. Ohno, H. Koinuma, M. Kawasaki, Nat. Mater. 4 (2005) 42.
[3] K. Yamanouchi, K. Kotani, H. Yao, Jpn. J. Appl. Phys. 37 (1998) 2887.
[4] P. Waltereit, O. Brandt, A. Trampert, H.T. Grahn, J. Menniger, M. Ramsteiner, M. Reiche, K.H. Ploog, Nature 406 (2000) 865.
[5] G. Vaschenko, D. Patel, C.S. Menoni, N.F. Gardner, J. Sun, W. Götz, C.N. Tomé, B. Clausen, Phys. Rev. B 64 (2001) 241308.
[6] T. Makino, A. Ohtomo, C.H. Chia, Y. Segawa, H. Koinuma, M. Kawasaki, Physica E 21 (2004) 671.
[7] J.Zuniga Perez, V.M. Sanjose, E.P. Lidon, J. Colchero, Phys. Rev. Lett. 95 (2005) 226105.
[8] O. Dulub, L.A. Boatner, U. Diebold, Surf. Sci. 519 (2002) 201.
[9] T. Koida, S.F. Chichibu, A. Uedono, T. Sota, A. Tsukazaki, M. Kawasaki, Appl. Phys. Lett. 84 (2004) 1079.
[10] J. Zuniga-Perez, V. Munoz-Sanjose, E. Palacios-Lidon, J. Colchero, Appl. Phys. Lett. 88 (2006) 261912.
[11] T. Moriyama, S. Fujita, Jpn. J. Appl. Phys. 44 (2005) 7919.
[12] H. Matsui, H. Tabata, Appl. Phys. Lett. 87 (2005) 143109.
[13] H. Matsui, H. Tabata, J. Appl. Phys. 99 (2006) 124307.
[14] Mitch M.C. Chou, S.J. Huang, C.W.C. Hsu, J. Crystal Growth 203 (2007) 585.
[15] Mitch M.C. Chou, H.C. Huang, D.S. Gan, C.W.C. Hsu, J. Crystal Growth 291 (2006) 485.
[16] L.A. Giannuzzi, F.A. Stevie, Micron 30 (1999) 197.
[17] K. Vanheusden, W.L. Warren, C.H. Seager, D.R. Tallant, J.A. Voigt, B.E. Gnade, J. Appl. Phys. 79 (1996) 7983.